SCIENTIFIC BRIEFING

HP TODAY

HYDROLOGICAL PROCESSES
Hydrol. Process. **26**, 3312–3318 (2012)
Published online 3 July 2012 in Wiley Online Library (wileyonlinelibrary.com). DOI: 10.1002/hyp.9424

Difference infiltrometer: a method to measure temporally variable infiltration rates during rainstorms

John A. Moody* and Brian A. Ebel

U.S. Geological Survey, National Research Program, Boulder, CO, USA

*Correspondence to:
John Moody, National Research Program, U.S. Geological Survey, 3215 Marine Street, Suite E-127, Boulder, Colorado 80303, USA.
E-mail: jamoody@usgs.gov

Received 10 April 2012
Accepted 21 May 2012

Abstract

We developed a difference infiltrometer to measure time series of non-steady infiltration rates during rainstorms at the point scale. The infiltrometer uses two, tipping bucket rain gages. One gage measures rainfall onto, and the other measures runoff from, a small circular plot about 0.5-m in diameter. The small size allows the infiltration rate to be computed as the difference of the cumulative rainfall and cumulative runoff without having to route water through a large plot. Difference infiltrometers were deployed in an area burned by the 2010 Fourmile Canyon Fire near Boulder, Colorado, USA, and data were collected during the summer of 2011. The difference infiltrometer demonstrated the capability to capture different magnitudes of infiltration rates and temporal variability associated with convective (high intensity, short duration) and cyclonic (low intensity, long duration) rainstorms. Data from the difference infiltrometer were used to estimate saturated hydraulic conductivity of soil affected by the heat from a wildfire. The difference infiltrometer is portable and can be deployed in rugged, steep terrain and does not require the transport of water, as many rainfall simulators require, because it uses natural rainfall. It can be used to assess infiltration models, determine runoff coefficients, identify rainfall depth or rainfall intensity thresholds to initiate runoff, estimate parameters for infiltration models, and compare remediation treatments on disturbed landscapes. The difference infiltrometer can be linked with other types of soil monitoring equipment in long-term studies for detecting temporal and spatial variability at multiple time scales and in nested designs where it can be linked to hillslope and basin-scale runoff responses. Published 2012. This article is a U.S. Government work and is in the public domain in the USA.

Key words wildfire; infiltration; Fourmile Canyon; convective and cyclonic storms; runoff

Introduction

Predicting runoff from ungaged basins is especially difficult when a basin has been burned by wildfire that can change soil properties. Infiltration rates or 'effective rainfall rates' are a critical input into predictive models of runoff whether the basin is unburned or burned. Ring infiltrometers, drip infiltrometers, rainfall simulators, and tension infiltrometers are some methods that have been used to measure infiltration (e.g. Youngs, 1991; Smettem and Smith, 2002) at essentially the point scale of about 1 m^2 or less. All have the disadvantage of using some type of artificial wetting of the soil under constant conditions that do not simulate the spatial, temporal, and drop size variability of natural rainfall. Moreover, the wetting of a small, isolated region of the soil also commonly requires corrections for subsurface lateral spreading. Ring infiltrometers use ponded water to apply a constant head (Johnson, 1963; Talsma, 1969) as do some disc permeameters (Talsma and Hallam, 1980; Perroux and White, 1988), and some use a falling head (Nimmo *et al.*, 2009). Results for these ring-type infiltrometers for soils affected by wildfire indicate that measurements of saturated hydraulic conductivity, K_{sat} [mm h^{-1}], are often greater than those measured by using other methods because the positive pressure heads (5–6 cm) may overwhelm the factors that reduce K_{sat} in burned soils (Cerdà, 1996; Nyman *et al.*, 2010; Ebel *et al.*, 2012). Tension infiltrometers avoid this problem and

measure infiltration rates for water applied at negative pressure heads (Perroux and White, 1988; Decagon, 2006; Robichaud *et al*., 2008; Moody *et al*., 2009) but frequently are difficult to interface with the soil surface requiring that material be added to the soil surface to provide good contact. Rainfall simulators are among the most commonly used infiltration methods described in the literature for unburned and burned soils ranging in size from portable to truck-supported systems (Kinner and Moody, 2008). They use either a drip system (McQueen, 1963; Selby, 1970; Martin and Moody, 2001) or spray nozzle (fixed, multiple, or oscillating) system (Wilcox *et al*., 1986; Dunne *et al*., 1991; Cerdà *et al*., 1997; Benavides-Solorio and MacDonald, 2001; Pierson *et al*., 2001; Kinner and Moody, 2008) to simulate rain. Simulators avoid the problems of the constant or falling head methods and the interfacing problem but commonly use constant rainfall intensities—some of which are not physically realistic and some do not have drop-size distributions, kinetic energies, or temporal variations representative of natural rain (Renard, 1985).

Rainfall and runoff have been measured at the plot scale (10–100 m^2) using tipping bucket gage technology for years (e.g. Peters *et al*., 1995; Coelho *et al*., 2004; Ferreira *et al*., 2005), but at this larger scale, the additional non-trivial uncertainty in the water routing processes makes it challenging to reliably measure temporally variable infiltration and runoff in response to natural rainfall. This technical note describes the difference-infiltration method for measuring temporally variable infiltration rates during natural rainfall by using paired, tipping bucket gages at the point scale (1 m^2) where water routing can be neglected and the vertical flux in the subsurface can be assumed to be one-dimensional because natural rainfall also wets the region outside the infiltrometer plot. These time series of infiltration rate can be combined with measurements of the initial soil-water content and soil properties to estimate K_{sat} using relatively simple infiltration models (e.g. Green and Ampt, 1911; Philip, 1957) or a full numerical solution to Richards equation (Šimùnek *et al*., 2008).

Methods

Infiltration rates

Time variable infiltration rates are computed from a time series of rainfall and a time series of runoff from a bounded plot measured by using two, tipping-bucket rain gages. The two gages and the plot are referred to in this paper as a difference infiltrometer, and two difference infiltrometers (DI-1 and DI-2) were deployed on a north-facing slope severely burned by the 2010 Fourmile Canyon Fire. This field site is about 10 km west of Boulder, Colorado, in the Front Range mountains (Ebel *et al*., 2012; Moody and Ebel, 2012). DI-1 was deployed near the crest of a hillslope and had a slope of 15°, and DI-2 was located further downhill where the slope was 24°. The two, tipping-bucket rain gages (Onset Computer Corp. Model RG2) had 15.3-cm, inside diameter entrance funnels and recorded the time of each tip (0.254 mm) using a HOBO event logger (Onset Computer Corp.). Each tipping bucket was calibrated in the laboratory at 6 different 'standard' intensities, ranging from 7 to 100 mm h^{-1}, using a peristaltic pump to control the drip or rain rate delivered to the gages. Runoff from small bounded hillslope plots (~0.5- to 0.8-m diameter, 0.25–0.50 m^2; Figure 1A) was collected on the downhill side of the nearly circular plot and directed through a 1.5-cm diameter semi-rigid plastic delivery pipe into the runoff gage with a 16-cm diameter plastic cap to prevent rainfall from entering the runoff gage (Figure 1B). A 1-mm nylon mesh screen was added on top of the existing wire screen (with 3-mm diameter holes) inside the funnel to reduce the amount of debris entering the runoff gage. Each runoff gage was checked and cleaned 2–3 times per week, and the delivery pipe was cleaned by using a small bottle brush to ensure that there was no blockage before the next rainstorm. A larger diameter pipe could be used to reduce the possibility of blockage before and during a storm but will not replace regular maintenance to ensure reliable data. Data were downloaded from the rainfall and runoff gages every 1–2 weeks so that the clock drift in the data loggers would be minimal. Drifts were on the order of 3–7 s d^{-1}.

Observed time-variable infiltration rates were calculated from the difference between the cumulative rainfall and the cumulative runoff time series. Tipping-bucket rain gages only record the time of the first tip and not the time at which the rain started. Therefore, the time and cumulative rain and runoff corresponding to the first three tips were used to extrapolate back in time to an estimated start time for the rain and the runoff. Rainfall and runoff cumulative curves had values at irregular time intervals, so they were digitized by using piece-wise linear interpolation to a regular interval that was a multiple of 0.1 or 0.25 min and that was closest to 0.1 x the average tip interval of the storm, Δt (total time divided by total number of tips). Average tip intervals of the runoff gage were always less than that those for the rain gage because the runoff gage had a larger collecting area. The difference of these two cumulative curves (rainfall minus runoff) was the observed cumulative infiltration curve. Based on Δt, the rainfall, runoff, and infiltration rates were computed as a backwards difference equal to the total rainfall in an accumulation interval lasting $0.5\Delta t$ (but not less than 1 min) and ending at the desired time. These accumulation values were then converted to an equivalent rate of mm h^{-1}. Positive values of the difference between rainfall and runoff rates would represent surface wetting, surface storage in depressions, and infiltration, whereas negative values could represent draining of depression storage and, if present, return flow from the subsurface. The fact that the two buckets tip at different times introduces some noise in the data processing.

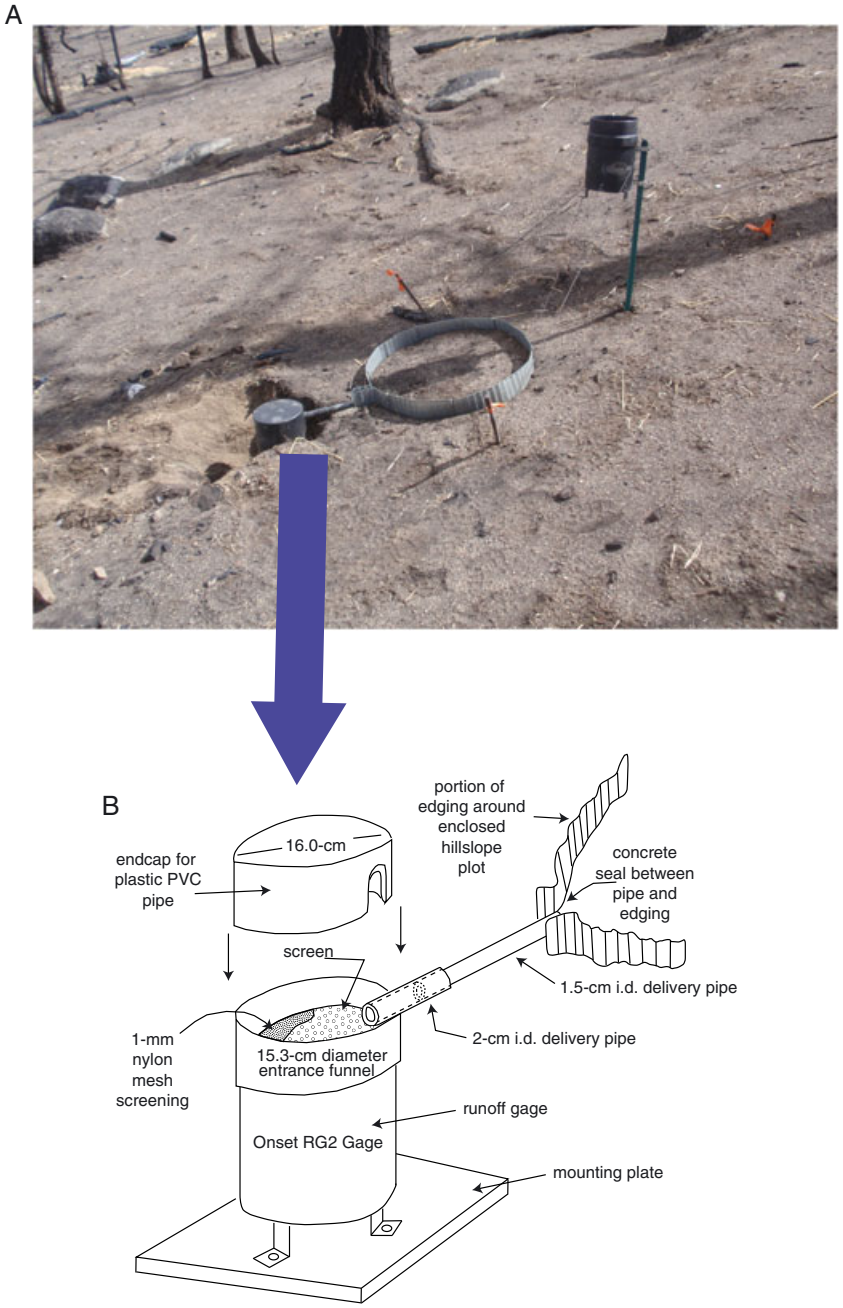

Figure 1. A. Difference infiltrometer with rain gage in the upper right on the post, ~0.5-m diameter bounded hillslope plot in the center, and runoff gage in the lower left. Edging around the plot was pushed into the soil to a depth of 1–2 cm. B. Expanded view showing details of runoff gage deployment

Estimates of saturated hydraulic conductivity

We estimated K_{sat} using an inverse solution in the Hydrus 1-D software package (Šimùnek *et al.*, 2008). Van Genuchten (1980) parameters were estimated with the software RETC (van Genuchten *et al.*, 1991) fit to soil-water retention data measured in the laboratory (Daniel B. Stevens, Albuquerque, New Mexico) on intact 6-cm diameter cores collected near the difference infiltrometer plots. Initial conditions (i.e. soil–water content) at the surface were measured periodically (2–3 times per week) using thermo-gravimetric methods (Topp and Ferré, 2002) on near-surface cores (3-cm deep; 4.7-cm diameter). Initial conditions at depth were measured at 5, 10, 15, and 20 cm below the surface with soil–water content sensors (Decagon Devices, 5TE), which sampled at 1-min time interval and were calibrated using soil that was collected near the difference infiltrometer plots. The inverse solution for K_{sat} was found by minimizing the sum of the squared differences between the observed and predicted infiltration rate during the period of runoff.

Results and Discussion

Operating conditions

The area of the difference infiltrometer plots was designed to be about ten times the entrance diameter of the rain gage to

prevent the runoff from the plot from exceeding the capacity of the runoff gage. The capacity of each tipping-bucket in the rain and runoff gages is 4.73 cm^3. If the difference infiltrometer is exposed to a 5-min rainfall intensity equal to 100 mm h^{-1} (this is approximately the 100-year recurrence frequency for the area where the difference infiltrometer was deployed, Miller *et al.*, 1973) and assuming a runoff ratio of 0.5, the expected runoff rate from the plot would be 2.6 cm^3 s^{-1}, well below the capacity of the tipping-bucket gage. However, if the runoff coefficient was 1, then this plot size would exceed the capacity of the gage (4.7 cm^3). In our study, the actual plot areas, when actually installed were greater than the intended area to accommodate rocks in the near-surface soil and ranged from 14 to 27 times larger than the rain gage entrance diameter. Therefore, the capacity for these difference infiltrometers may be exceeded if 5-min rainfall intensities are greater than 100 mm h^{-1}. This could limit the operational range of the difference infiltrometer for the runoff plot configuration of this specific deployment but only for storms with intensities greater than 100 mm h^{-1}, which are rare. Records for a few storms did show possible truncated peaks for maximum 5-min intensity, I_5 [mm h^{-1}] equal to 70 mm h^{-1}, probably caused by the limited amount of flow that can pass through the 1.5-cm diameter delivery pipe. Plot size or pipe diameter could be easily adjusted to match expected rainfall–runoff characteristics for a given location.

Magnitude of possible errors

The calibration relation between the 'standard' rainfall intensities (pump rates) and the rainfall intensities measured by the tipping-bucket rain gage were linear with coefficient of determination, R^2, ranging from 0.9972 to 0.9996. Tipping-bucket rain gages tend to underestimate the rainfall intensity, which is corrected for by the slope of the calibration equation, which for the four rain gages were 1.103 and 1.108 for DI-1 and 1.027 and 1.080 for DI-2. The average variability (coefficient of variation) of the seven standard rainfall intensities ranged from 0.5 to 2.2%, and the average variability of the rain gage intensities ranged from 2.2 to 3.5%.

Runoff contains some sediment but the error in the measured rainfall intensity is minimal. For example, assuming a suspended-sediment concentration of 1000 mg l^{-1} would change the mass of water in the tipping bucket (equivalent to 4.73 cm^3) and, thus, the rain intensity by 0.1%. Particles not in suspension that pass through the nylon mesh and wire screens could be as large as 1 mm in diameter, and ten of these particles would change the mass of the water and sediment (assuming a density of 2.65 g cm^{-3}) in the tipping bucket such that the increase in rainfall intensity would be 0.3%. Both sources of sediment are either removed or washed out with each tip of the rain gage so that there is no accumulation error.

Error in the water balance can depend on the accumulation interval used to compute the rainfall intensity or rate. If the accumulation interval is less than the duration of the rainfall then the error is on the order of 0–3%. It is 2–3% if the accumulation interval is less than the elapsed time from the estimated start of the rainfall to the time of the first tip of the gage. This is because we approximated the increase in rainfall rate (i.e. the acceleration of the rainfall) as being linear from the start of the rainfall to the time of the first tip rather than as a constant rainfall intensity, which is the case when the cumulative rainfall is linearly interpolated. Accumulation intervals equal to or greater than the duration should not be used because they can result in substantial errors, for example, as large as 25–50% for durations of 34 and 20 min, respectively, based on some hyetographs we measured. These errors also apply to the infiltration rate because it equals the difference between rainfall intensity and runoff discharge.

Infiltration rates and saturated hydraulic conductivity

As examples of the method and for the sake of brevity, we present infiltration rates estimated by using cumulative rainfall and runoff curves for only two storms from just one of the two difference infiltrometers (DI-1) deployed on the north-facing slope between 19 June and 14 September 2011 (12 other runoff events for DI-1 and 18 runoff events for DI-2 are not presented in this paper). Runoff was frequently produced by individual rain cells within a rainstorm. One rain cell, with low-intensity rainfall, was imbedded in a cyclonic frontal storm on 7 September 2011 that had a long duration (7 h) and 15.7 mm of total rainfall. The other rain cell, with high-intensity rainfall, was imbedded in a convective storm on 10 July 2011, which had a short duration (35 min) and 7.6 mm of total rainfall. The antecedent volumetric soil water content in the top 3 cm of the soil (measured thermogravimetrically) was 0.019 cm^3 cm^{-3} before the 7 September storm and 0.083 cm^3 cm^{-3} before the 10 July storm.

Infiltration rates during the low-intensity cyclonic storm in September were measured after several hillslope erosional events. Infiltration was equal to the average rain intensity (0.8 mm h^{-1}) until runoff started 99.3 min after the start of the rain (Figure 2A). Infiltration rates during the storm ranged from 0 to 3.6 mm h^{-1} and were quite variable (Figure 2B). This variability may reflect the fluctuations of the water stored by the microtopography within the plot in response to fluctuations in rainfall. Based on the difference infiltrometer data, runoff began when the rainfall intensity exceeded 1.1 mm h^{-1}, and the cumulative rainfall was 1.4 mm. The inverse solution gave a preliminary estimate of K_{sat} for this storm cell of 0.20 ± 0.01 mm h^{-1}. Tension infiltrometer measurements (Decagon Devices, Minidisk) made during the previous fall of 2010 indicated an average K_{sat} of 10 ± 28 mm h^{-1}, which was less than the constant head (27 ± 4 mm h^{-1}) and the falling head (80–880 mm h^{-1}) permeameter values (Ebel *et al.*, 2012). These observations agree with the tendency of the constant or falling head

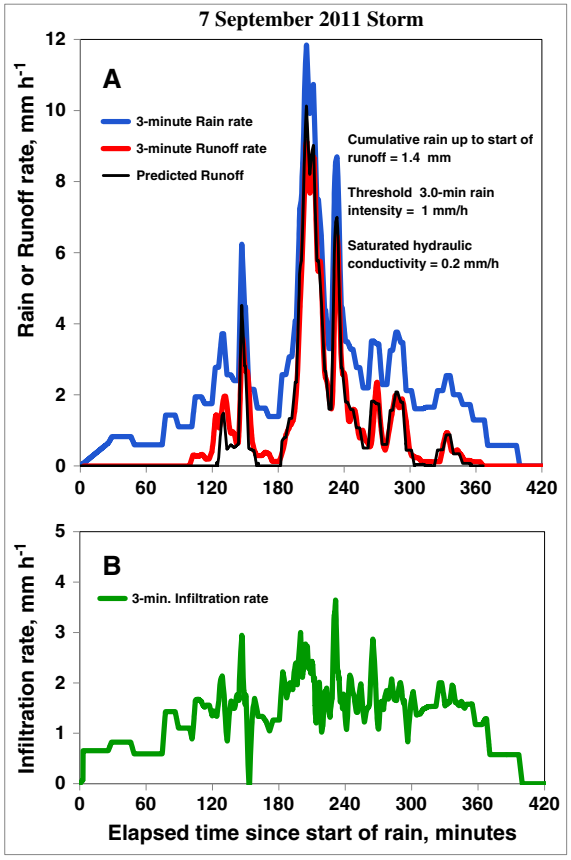

Figure 2. A. Measured rainfall and runoff rates for a long-duration, low-intensity cyclonic frontal storm cell on 7 September 2011, for which, there was about 1 tip of the rain gage per 6 min, so 3-min rates were computed. Predicted runoff is based on an inverse solution to estimate saturated hydraulic conductivity with the measured infiltration rates (during runoff) used in the objective function. Threshold 3.0-min rain intensity corresponds to the start of runoff. B. Calculated infiltration rates

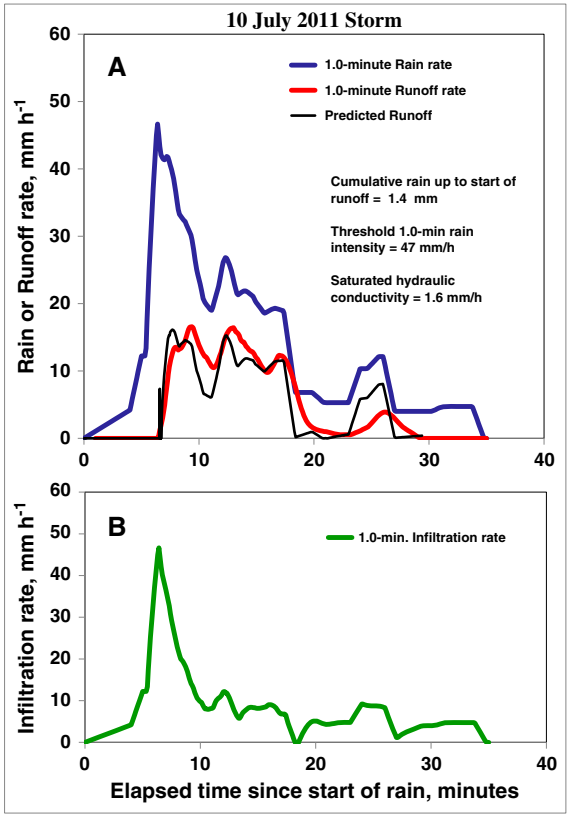

Figure 3. A. Measured rainfall and runoff rates for a short-duration, high-intensity convective storm cell on 10 July 2011, for which, there was about 1 tip of the rain gage per minute so 1.0-min rates were computed. Predicted runoff is based on an inverse solution to estimate saturated hydraulic conductivity with the measured infiltration rates (during runoff) used in the objective function. Threshold 1.0-min rain intensity corresponds to the start of runoff. B. Calculated infiltration rates

methods to estimate greater values of K_{sat} (Cerdà, 1996; Nyman *et al.*, 2010; Ebel *et al.*, 2012) than other methods.

Results for the convective storm during the summer (10 July 2011) before most of the major erosion events were quite different. Initial infiltration rate into the burned soil was equal to the rain intensity, which ranged from 0 to 51.6 mm h^{-1}. Runoff began at 7.4 min after the start of the rain and after the time of the peak rain intensity (Figure 3A). The rainfall intensity at the start of runoff was 46.7 mm h^{-1}, and the cumulative rainfall was 1.4 mm (same as the cyclonic storm). The preliminary estimate based on an inverse solution for K_{sat} using data for this storm cell was 1.59 ± 0.01 mm h^{-1}.

These two estimates of K_{sat} are less than values measured using either constant or falling head methods. These methods are known to overestimate K_{sat}, which for soils from a variety of burned severities and forest types throughout the world, are also greater and range from 30 to 855 mm h^{-1} (Robichaud, 2000; Neary, 2011). The implication of the lower values of K_{sat}, corresponding to natural rainfall is that burned areas will be more sensitive to runoff, flooding, and debris flows than previously suggested by the higher values of K_{sat}. Thus, these two examples suggest that using the difference infiltrometer may provide more accurate estimates of K_{sat}, for post-wildfire rainfall–infiltration–runoff prediction models.

Summary

The difference infiltrometer measures time series of non-steady infiltration rates during rain storms. Although the difference infiltrometers were used in burned basins, the method is suitable for unburned basins in any landscape. Tipping-bucket gages have been used for a long time to measure rainfall and runoff for large plots; however, infiltration cannot be measured directly for large plots without accounting for the travel time of the water. The small size of the plot used in the difference infiltrometer avoids this problem and is essential to the success of the method. The difference infiltrometer has several other advantages:

- uses readily available and relatively inexpensive instrumentation;
- is portable, requires transporting no water, and is easy to deploy in rugged and steep terrain;
- measures time variable infiltration rates corresponding to time variable rainfall during a rainstorm;

- can be used to measure K_{sat} under natural rainfall conditions and, thus, requires no correction for spreading outside the plot of the difference infiltrometer. This eliminates a source of uncertainty and, therefore, may provide better estimates of K_{sat};
- can be used for long-term monitoring of temporal changes in infiltration rates and soil properties;
- is ideal for paired experiments (treatment *versus* control) to measure the effectiveness of soil treatments under natural rainfall conditions, which are extremely difficult to reproduce;
- can be used to measure infiltration properties, validate infiltration models, and assess recovery of disturbed landscapes;
- can be used in conjunction with rainfall simulators. Simulators could be used to pre-wet soils to a desired initial condition within the difference infiltrometer plot, and the difference infiltrometer would then measure the response to natural, time-variable rainfall.

Additionally, it can be linked with other types of soil monitoring equipment in long-term studies for detecting temporal and spatial variability at multiple time scales and in nested designs where the difference infiltrometer can be linked to hillslope and basin-scale runoff responses.

Acknowledgements

Petter Nyman, Artemi Cerdà, and Jason Kean each provide timely and insightful suggestions relative to the interpretation of the data processing and details of the scientific briefing itself. Bob Stallard provided critical enthusiasm, encouragement, and additional comments. Brian Ebel received support from the Mendenhall Postdoctoral Fellowship Program in the National Research Program of the US Geological Survey. Any use of trade, firm, or product names is for descriptive purposes only and does not imply endorsement by the US Government.

KEY POINTS

- Paired rain gages measure rainfall and runoff from a bounded plot uphill.
- Small enough that it is portable and avoids water routing problems inherent to large plots.
- Measures non-steady infiltration rates during natural rather than artificial rainfall.
- Method can be used to monitor infiltration properties and validate models.

References

Benavides-Solorio J, MacDonald LH. 2001. Post-fire runoff and erosion form simulated rainfall on small plots, Colorado Front Range. *Hydrological Processes* **15**: 2931–2952.

Cerdà A. 1996. Seasonal variability of infiltration rates under contrasting slope conditions in southeast Spain. *Geoderma* **69**: 217–232.

Cerdà A, Ibáñez S, Calvo A. 1997. Design and operation of a small and portable rainfall simulator for rugged terrain. *Soil Technology* **11**: 163–170.

Coelho COA, Ferreira AJD, Boulet AK, Keizer JJ. 2004. Overland flow generation processes, erosion yields and solute loss following different intensity fires. *Quarterly Journal of Engineering Geology & Hydrogeology* **37**: 233–240.

Decagon. 2006. *Mini Disk Infiltrometers User's Manual*. Decagon Devices: Pullman, WA; 18.

Dunne T, Zhang W, Aubry BF. 1991. Effects of rainfall, vegetation and microtopography on infiltration and runoff. *Water Resources Research* **27**(9): 2271–2285.

Ebel BA, Moody JA, Martin DA. 2012. Hydrologic properties, states, and fluxes immediately after wildfire. *Water Resources Research* **48**: W03529, DOI: 10.1029/2011WR011470

Ferreira AJD, Coelho COA, Boulet AK, Leighton-Boyce G, Keizer JJ, Ritsema CJ. 2005. Influence of burning intensity on water repellency and hydrological processes at forest and shrub sites in Portugal. *Australian Journal of Soil Research* **43**: 327–336.

van Genuchten MT. 1980. A closed-form equation for predicting the hydraulic conductivity of unsaturated soil. *Soil Science Society of America Journal* **44**: 892–898.

van Genuchten MT, Leij FJ, Yates SR. 1991. The RETC code for quantifying the hydraulic functions of unsaturated soils, *EPA/600/2091/065*, Robert S. Kerr Environmental Research Laboratory, Office of Research and Development, U.S. Environmental Protection Agency, Ada, Oklahoma.

Green WH, Ampt GA. 1911. Studies on soil physics — Part I. The flow of air and water through soils. *Journal of Agricultural Science* **4**: 1–24.

Johnson AI. 1963. A field method for measurement of infiltration, *U.S. Geological Survey Water-Supply Paper 1544-F*; 27.

Kinner DA, Moody JA. 2008. Infiltration and runoff measurements on steep burned hillslope using a rainfall simulator with variable rain intensities. *Scientific Investigations Report 2007–5211*. U.S. Geological Survey; 64.

Martin DA, Moody JA. 2001. Comparison of soil infiltration rates in burned and unburned mountainous watersheds. *Hydrological Processes* **15**: 2893–2903, DOI: 10.1002/hyp.380

McQueen IS.1963. Development of a hand portable rainfall-simulator infiltrometer. *U.S. Geological Survey Circular 482*. U.S. Geological Survey, 16.

Miller JF, Frederick RH, Tracey RJ. 1973. Precipitation-frequency atlas of the western United States, Volume III—Colorado. *National Oceanic and Atmospheric Administration*, National Weather Service; 67.

Moody JA, Ebel BA. 2012. Hyper-dry conditions provide new insights into the cause of extreme floods after wildfire. *Catena* **93**: 58–63, DOI: 10.1016/j.catena.2012.01.006

Moody JA, Kinner DA, Ubeda X. 2009. Linking hydraulic properties of fire affected soils to infiltration and water repellency. *Journal of Hydrology* **379**: 291–303, DOI: 10.1016/j.jhydrol.2009.10.015

Neary DG. 2011. Impacts of Wildfire Severity on Hydraulic Conductivity in Forest, Woodland, and Grassland Soils. *Hydraulic Conductivity - Issues, Determination and Applications*. Prof. Lakshmanan Elango (Ed.), ISBN: 978-953-307-288-3, InTech, Available from: http://www.intechopen.com/books/hydraulic-conductivity-issues-determination-and-applications/impacts-of-wildfire-severity-on-hydraulic-conductivity-in-forest-woodland-and-grassland-soils

Nimmo JR, Schmidt KM, Perkins KS, Stock JD. 2009. Rapid measurement of field-saturated hydraulic conductivity for areal characterization. *Vadose Zone Journal* **8**: 142–149, DOI: 10.2136/vzj2007.0159

Nyman P, Sheridan G, Lane PNJ. 2010. Synergistic effects of water repellency and macropore flow on the hydraulic conductivity of a burned forest soil, south-east Australia. *Hydrological Processes* **24**: 2871–2887, DOI: 10.1002/hyp.7701.n

Perroux KM, White I. 1988. Designs for disc permeameters. *Soil Science Society of America Journal* **52**(5): 1205–1215.

Peters DL, Buttle JM, Taylor CH, LaZerte BD. 1995. Runoff production in a shallow soil Canadian Shield basin. *Water Resources Research* **31**: 1291–1304.

Philip JR. 1957.The theory of infiltration: 1. the infiltration equation and its solution. *Soil Science* **83**: 345–358.

Pierson FB, Robichaud PR, Spaeth KE. 2001. Spatial and temporal effects of wildfire on the hydrology of a steep rangeland watershed. *Hydrological Processes* **15**: 2905–2916.

Renard KG. 1985. Rainfall simulators and USDA erosion research: History, perspective, and future. In Lane LJ (editor) *Proceeding of the Rainfall Simulator Workshop*, January 14–15, 1985, Tucson, Arizona. 3–6.

Robichaud PR. 2000. Fire effects on infiltration rates after prescribed fire in Northern Rocky Mountain forests, USA. *Journal of Hydrology* **231–232**: 220–229, DOI: 10.1016/S0022-1694(00)00196-7

Robichaud PR, Lewis SA, Ashmun LE. 2008. New procedure for sampling infiltration to assess post-fire water repellency. USDA Forest Service *Research Note RMRS-RN-33*, U.S. Forest Service; 14.

Selby MJ. 1970. Design of a hand-portable rainfall-simulating infiltrometer, with trial results from the Otutira catchment. *Journal of Hydrology, New Zealand* **9**(2): 117–132.

Šimùnek J, van Genuchten MT, Šejna M. 2008. Development and applications of the HYDRUS and STANMOD software packages and related codes. *Vadose Zone Journal* **7**: 587–600, DOI: 10.2136/VZJ2007.0077

Smettem KRJ, Smith RE. 2002. Field measurement of infiltration parameters, *in* Smith, R.E. (ed.), American Geophysical Union. *Water Resources Monograph* **15**: Chap. 8, 135–157.

Talsma T. 1969. In situ measurement of sorptivity. *Australian Journal Soil Research.* **7**: 269–276.

Talsma T, Hallam PM. 1980. Hydraulic Conductivity measurement of forest catchments. *Australian Journal Soil Research.* **30**: 139–148.

Topp GC, Ferré PA. 2002. Methods for measurement of soil water content: Thermogravimetric using convective oven-drying. In *Methods of Soil Analysis. Part 4 Physical Methods*, Dane JH, Topp GC (eds). Soil Science Society of America Book Series: 5, Soil Science Society of America: Madison, WI; 422–424.

Wilcox BP, Wood MK, Tromble JT, Ward TJ. 1986. A hand-portable single nozzle rainfall simulator designed for use on steep slopes. *Journal of Range Management* **39**(4): 375–377.

Youngs EG. 1991. Infiltration Measurements-A Review. *Hydrological Processes* **5**: 309–320.

